

No Forgetting Learning: Memory-free Continual Learning

Mohammad Ali Vahedifar

Qi Zhang

Abstract

Continual Learning (CL) remains a central challenge in deep learning, where models must sequentially acquire new knowledge while mitigating Catastrophic Forgetting (CF) of prior tasks. Existing approaches often struggle with efficiency and scalability, requiring extensive memory or model buffers. This work introduces “No Forgetting Learning” (NFL), a memory-free CL framework that leverages knowledge distillation to maintain stability while preserving plasticity. Memory-free means the NFL does not rely on any memory buffer. Through extensive evaluations of three benchmark datasets, we demonstrate that NFL achieves competitive performance while utilizing approximately 14.75 times less memory than state-of-the-art methods. Furthermore, we introduce a new metric to better assess CL’s plasticity-stability trade-off.

1. Introduction

Neural Networks (NNs) trained sequentially on multiple tasks often suffer from catastrophic Forgetting (CF) [39], where new learning disrupts previously acquired knowledge. This challenge is rooted in the plasticity-stability dilemma—while NNs exhibit high plasticity, enabling rapid adaptation, they often lack the stability required to preserve past information [27, 36]. As a result, performance on earlier tasks deteriorates over time [35]. Continual Learning (CL) provides a framework to mitigate CF, allowing NNs to learn sequentially while retaining prior knowledge without storing or revisiting past data [17]. It is also known as lifelong, sequential, or incremental learning. CL enables models to generalize across dynamically evolving tasks and domains [26], making it essential for real-world Artificial Intelligence (AI) systems that operate in non-stationary environments. Various approaches have been developed to address CF in CL. For an algorithm to be considered a CL method, it must adhere to several key criteria:

1. **Balanced Learning:** The model should maintain performance across both previously learned and newly introduced classes, preventing overfitting to recent tasks [42].
2. **Learning from Stream of Data Sets:** The algorithm

should be capable of learning from a stream of data sets with more recent data sets introducing new classes [30].

3. **Consistent Multi-Class Classification:** At any stage, the model should accurately classify all learned classes. [3].
4. **Scalability and Efficiency:** Computational and memory overhead should remain stable or grow minimally with the number of tasks. Many existing methods rely on *memory buffers* to store and retrieve data from previous tasks, which represents a clear weakness as it violates the strict CL setting, where no prior task data should be accessible [3, 30].

Many existing CL methods do not fully comply with these criteria [17, 33, 44, 45]. As demonstrated in [35, 50], dynamic architectures [8, 32, 43] and memory-based [2, 23, 30] approaches often require additional storage, making them difficult to compare fairly with *memory-free* techniques like Knowledge Distillation (KD) and regularization-based methods [35, 50]. Similarly, memory-based replay methods outperform others due to direct access to prior samples, creating inherent benchmarking inconsistencies. Each method has its own pros and cons; selecting the right method depends on the application and resource constraints.

This paper introduces a novel CL method, *No Forgetting Learning (NFL)*, along with its enhanced version, NFL+. These methods extend the KD technique [3, 22, 29, 30, 42] while ensuring a memory-free (without access to a memory buffer) learning paradigm. NFL preserves previously learned knowledge by leveraging shared parameters across tasks, facilitating robust adaptation to new tasks without CF. NFL+ further enhances feature retention through an Auto-Encoder (AE) and mitigates bias in the final layer, ensuring stable performance across evolving task distributions. Unlike memory-buffer-dependent approaches [2, 3, 30], NFL does not store any past exemplars, making it scalable for real-world CL applications. By exploiting inter-class relationships, the NFL maintains knowledge consistency while learning new classes, effectively addressing the plasticity-stability trade-off.

The rest of this paper is structured as follows: Section 2 reviews related work. Section 3 presents the proposed NFL

framework and its variants, NFL+. Section 4 provides extensive experimental evaluations against state-of-the-art CL methods and additional insights into the CL paradigm. Finally, conclusions are provided in Section 5. Also, we provide a supplementary material 6 in the appendix, detailing further experimental results.

2. Related Work

Numerous methods leverage KD to mitigate CF by designating a previous version of the model as a *teacher*, which guides the current model as a *student* [15, 21, 31, 38, 39, 41, 42, 46]. KD [14] is a technique used to transfer knowledge from a teacher model to a student model. This is achieved by having the student model learn from targets provided by the teacher model, thereby capturing nuanced patterns that enhance the student model’s generalization ability [11]. This can be done by using new training samples [16, 22, 29], a limited set of old training samples [4, 7, 15, 30], unlabeled external data [21], or generated data by the model as it learns new tasks [41, 46]. ExpertGate [1] employs task-specific experts but struggles with expert selection for unseen inputs. Learning without Memorizing (LwM) [6] preserves classifier attention maps using Attention Distillation Loss. Encoder-Based Lifelong Learning (EBLL) [29] utilizes task-specific autoencoders for knowledge retention, though it increases model complexity. These approaches attempt to mitigate the distribution shift problem, although they are still experiencing this issue to some extent.

Among early approaches, Learning without Forgetting (LwF) [22] introduced a method to integrate new tasks while preserving knowledge from previous ones. LwF utilizes a shared convolutional network across tasks, modifying cross-entropy loss to retain prior predictions. While effective, it struggles with performance drops when new tasks come from different distributions. The Incremental Classifier and Representation Learning (iCaRL) [30] demonstrates that LwF suffers from error accumulation in sequential learning scenarios where data originates from the same distribution. iCaRL attempts to mitigate these issues by storing a subset of data from previous tasks. Similarly, Dark Experience Replay++ (DER++) [3] enhances knowledge retention by combining KD with cross-entropy loss to maintain inter-class relationships. CO-transport for class Incremental Learning (Coil) [47] proposes implementing bidirectional distillation through co-transport, leveraging the semantic relationships between the previous and updated models to enhance knowledge retention and transfer. Despite their effectiveness, KD-based methods that rely on memory buffers raise concerns regarding data privacy, memory efficiency, and computational overhead. These constraints make them impractical for applications with strict storage limitations or regulations prohibiting exemplar storage.

Reinforced Memory Management (RMM) [24], End-to-End Incremental Learning (EEIL) [4], LUCIR [15], PODNet [7], and MetaSP [34] attempt to balance memory use and knowledge retention, but they still fundamentally depend on exemplar replay, making them unsuitable for privacy-sensitive applications. Dynamic network-based methods like Memory-efficient Expandable Model (MEMO) [48] tackle memory constraints in CL by expanding models efficiently. MEMO observes shallow layers across tasks remain similar, whereas deeper layers require greater adaptation, optimizing network expansion with minimal resource overhead. However, a key drawback of dynamic networks is their reliance on additional model buffers, which increases computational and storage overhead over time.

3. No Forgetting Learning

We advocate that CL methods should ideally avoid accessing data from previous tasks entirely. With this in mind, we develop NFL assuming no access to data from previous tasks. Instead, NFL introduces a straightforward optimization process for training by leveraging the NN parameters trained on the NN on earlier tasks. In NFL+, we incorporate an AE and apply bias correction using encoded representations for the fully connected layer. While NFL+ requires additional computational resources, it delivers significant performance improvements.

3.1. NFL

Let us assume that a NN_1 has been trained on a dataset $D_t(X_t, Y_t)$ describing a task T_t formed by c_t classes in the class set \mathcal{C}_t . X_t denotes the data samples, each followed by a class label belonging to one of the c_t classes, and Y_t is the matrix formed by the one-hot class vectors corresponding to the targets for training the NN_1 . Let us also denote by θ_s all parameters of the NN_1 except the parameters of its last layer and the parameters of the last layer denoted by θ_t . The outputs of the NN_1 with randomly initialized θ_s^r and θ_t^r for X_t are given by (See part (1) of Fig. 1):

$$NN_1(X_t, \theta_s^r, \theta_t^r) \rightarrow \langle O_t^1, (\theta_s, \theta_t) \rangle. \quad (1)$$

The subscript in the output (i.e., O) denotes which set of classes are being learned, and the superscript indicates step numbering. r in the superscript of the parameters (i.e., θ) indicates random initialization. For this step, we calculate the following loss function.

$$\mathcal{L}_1 = \mathbb{E} \left[\mathcal{L}_{CE} \left(Y_t, O_t^1 \right) \right]. \quad (2)$$

Here, CE stands for cross-entropy loss function. After training the NN_1 on the dataset $D_t(X_t, Y_t)$, a new dataset $D_{t+1}(X_{t+1}, Y_{t+1})$ describing a new task T_{t+1} is obtained and we aim to train a new NN model that can achieve

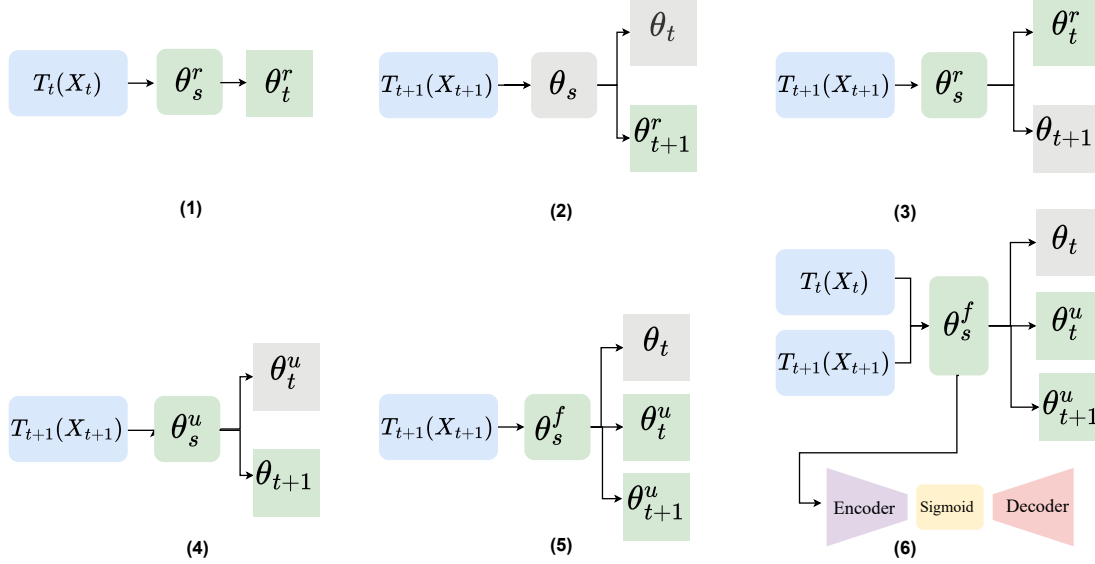


Figure 1. A Conceptual Illustration of NFL.

high performance on the combined task $T = T_t \cup T_{t+1}$ formed by c classes in the class set $\mathcal{C} = \mathcal{C}_t \cup \mathcal{C}_{t+1}$ classes, without access to the data and targets of the old dataset $D_t(X_t, Y_t)$. NFL follows a five-step process, summarized in Algorithm 1.

In step one, we introduce the data samples X_{t+1} to the trained NN_1 to obtain the logits (i.e., the outputs of the NN_1 before the softmax activation of the last layer):

$$\text{NN}_1(X_{t+1}, \theta_s, \theta_t) \rightarrow H_t. \quad (3)$$

These outputs will be used as *soft targets* for the new data samples X_{t+1} , providing knowledge concerning the old task T_t and preserving properties of the NN_1 leading to high performance on T_t .

For step two, we train the second NN_2 , where we freeze θ_s and θ_t obtained by Eq. 1 alongside training on randomly initialized θ_{t+1}^r until convergence, where the underline indicates freeze part (See part (2) of Fig. 1). The outputs of step two are obtained by:

$$\text{NN}_2(X_{t+1}, \theta_s, \theta_{t+1}^r) \rightarrow \langle O_{t+1}^2, (\theta_s, \theta_{t+1}) \rangle. \quad (4)$$

In this step, we calculate the following loss function.

$$\mathcal{L}_2 = \mathbb{E} \left[\mathcal{L}_{\text{CE}}(Y_{t+1}, O_{t+1}^2) \right]. \quad (5)$$

Here, Y_{t+1} denotes ground true labels for task T_{t+1} classes.

For step three, we train the third NN_3 model using the output parameters θ_{t+1} from the step two (See part (3) of Fig 1). The outputs of step three are obtained by:

$$\begin{aligned} \text{NN}_3(X_{t+1}, \theta_s^r, \theta_t^r, \theta_{t+1}) \rightarrow \\ \langle O_t^3, (\theta_s^u, \theta_t^u) \rangle; \langle O_{t+1}^3, (\theta_s^u, \theta_{t+1}^u) \rangle, \end{aligned} \quad (6)$$

where u in the superscript of the parameters (i.e., θ) indicates an updated version. For this step, we calculate the following loss function:

$$\mathcal{L}_3 = \mathbb{E} \left[\mathcal{L}_{\text{KD}}(H_t, O_t^3) + \lambda \mathcal{L}_{\text{CE}}(Y_{t+1}, O_{t+1}^3) \right], \quad (7)$$

where KD stands for KD loss function, and λ is a hyperparameter. The KD loss \mathcal{L}_{KD} is defined as follows:

$$\mathcal{L}_{\text{KD}}(h_k, o_k) = -\mathcal{H}(h'_k, o'_k) = -\sum_{i=1}^l h_k^{(i)} \log o_k^{(i)}, \quad (8)$$

where \mathcal{H} is the entropy and h'_k and o'_k are the modified versions of recorded and current probabilities h_k and o_k :

$$h_k^{(i)} = \frac{\left(h_k^{(i)}\right)^{1/p}}{\sum_j \left(h_k^{(j)}\right)^{1/p}} \quad (9)$$

$$o_k^{(i)} = \frac{\left(o_k^{(i)}\right)^{1/p}}{\sum_j \left(o_k^{(j)}\right)^{1/p}}. \quad (10)$$

In this context, p represents a temperature parameter used to control the smoothness of the probability distribution, with values typically set to $p > 1$ [14].

For step four, we train the fourth NN_4 model, where we use the outputs of the previous step after training by Eq. 6, then we fine-tune the θ_s^u and θ_{t+1}^u , simultaneously (See part (4)

of Fig. 1).

$$\begin{aligned} \text{NN}_4(X_{t+1}, \theta_s^u, \theta_t^u, \theta_{t+1}) \rightarrow \\ < O_t^4, (\theta_s^f, \theta_t^u) >; < O_{t+1}^4, (\theta_s^f, \theta_{t+1}^u) >, \end{aligned} \quad (11)$$

where, f in the superscript of the parameters (i.e., θ) indicates a fine-tuned version. For this step, we calculate the loss function as follows:

$$\mathcal{L}_4 = \mathbb{E} \left[\mathcal{L}_{\text{KD}}(H_t, O_t^4) + \omega \mathcal{L}_{\text{CE}}(Y_{t+1}, O_{t+1}^4) \right], \quad (12)$$

where ω is a hyperparameter. For step five, we calculate new target logits where we utilize the stored θ_t from step 1. New logits can be calculated by the following:

$$\text{NN}_5(X_{t+1}, \theta_s^f, \theta_t) \rightarrow \tilde{H}_t. \quad (13)$$

For the last step, we train the fifth NN_5 model, on the new dataset to learn from the new data with two logit targets (See part (5) of Fig 1). The outputs are calculated as follows:

$$\begin{aligned} \text{NN}_5(X_{t+1}, \theta_s^f, \theta_t, \theta_t^u, \theta_{t+1}^u) \rightarrow < O_t^5, (\theta_s^{f+}, \theta_t) >; \\ < O_t^5, (\theta_s^{f+}, \theta_t^f) >; < O_{t+1}^5, (\theta_s^{f+}, \theta_{t+1}^f) >, \end{aligned} \quad (14)$$

where $f+$ in the superscript of the parameters (i.e., θ) indicates a further fine-tuning. For this step, we calculate the following loss function:

$$\begin{aligned} \mathcal{L}_5 = \mathbb{E} \left[\alpha \mathcal{L}_{\text{KD}}(H_t, O_t^5) + (1 - \alpha) \mathcal{L}_{\text{KD}}(\tilde{H}_t, O_t^5) \right. \\ \left. + \beta \mathcal{L}_{\text{CE}}(Y_{t+1}, O_{t+1}^5) \right], \end{aligned} \quad (15)$$

where α and β are hyperparameters. The Eq. 14 outputs will be the share parameters (θ_s^{f+}) and task-specific parameters ($\theta_t^f, \theta_{t+1}^f$) for the next task.

3.2. NFL+

Let us assume the same setup as the NFL for training NFL+. The NFL+ improves the NFL's performance in six steps as outlined in Algorithm 2. At the start of training for the new task, the model's feature extractor, θ_s , has already been optimized for the previous task. A typical feature extraction (share parameters) approach would keep this component unchanged to preserve the performance of the previous task. However, this strategy limits the learning capability for a new task. Instead, our approach focuses on retaining only the features most relevant to the previous tasks while allowing flexibility for the rest, improving the model's ability to adapt to the new task. We use an AE trained on the previous task's data representations to achieve this. NFL+ employs an AE [10] on the representations of the first task's data derived from an optimized model to encode and preserve essential task-specific features by learning from the

Algorithm 1: No Forgetting Learning (NFL)

Inputs: Dataset $D_{t+1}(X_{t+1}, Y_{t+1})$ describing T_{t+1} , Parameters $\{\theta_s, \theta_t\}$ trained on T_t

Step 1: Train NN_1 with \mathcal{L}_1 from Eq. 2, calculate Soft Targets with Eq. 3

$$\text{NN}_1(X_t, \theta_s^r, \theta_t^r) \rightarrow < O_t^1, (\theta_s, \theta_t) >$$

Step 2: Train NN_2 with \mathcal{L}_2 from Eq. 5

$$\text{NN}_2(X_{t+1}, \theta_s, \theta_{t+1}^r) \rightarrow < O_{t+1}^2, (\theta_s, \theta_{t+1}) >$$

Step 3: Train NN_3 with \mathcal{L}_3 from Eq. 7

$$\begin{aligned} \text{NN}_3(X_{t+1}, \theta_s^r, \theta_t^r, \theta_{t+1}^r) \rightarrow \\ < O_t^3, (\theta_s^u, \theta_t^u) >; < O_{t+1}^3, (\theta_s^u, \theta_{t+1}^u) > \end{aligned}$$

Step 4: Train NN_4 with \mathcal{L}_4 from Eq. 12

$$\begin{aligned} \text{NN}_4(X_{t+1}, \theta_s^u, \theta_t^u, \theta_{t+1}^u) \rightarrow \\ < O_t^4, (\theta_s^f, \theta_t^u) >; < O_{t+1}^4, (\theta_s^f, \theta_{t+1}^u) > \end{aligned}$$

Step 5: Compute new logits with Eq. 13, Train NN_5 with \mathcal{L}_5 from Eq. 15

$$\begin{aligned} \text{NN}_5(X_{t+1}, \theta_s^f, \theta_t, \theta_t^u, \theta_{t+1}^u) \rightarrow < O_t^5, (\theta_s^{f+}, \theta_t) >; \\ < O_t^5, (\theta_s^{f+}, \theta_t^f) >; < O_{t+1}^5, (\theta_s^{f+}, \theta_{t+1}^f) > \end{aligned}$$

Output: Share Parameters $\{\theta_s^{f+}\}$, Task Specific Parameters $\{\theta_t^f, \theta_{t+1}^f\}$ for the next task

extracted features of each task. The AE function is formally defined as:

$$R(X_t) = W_{\text{Dec}} \sigma(W_{\text{Enc}} X_t). \quad (16)$$

Here W_{Enc} is encoder weights, W_{Dec} is decoder weights, σ is the activation function. By regulating the distance between the reconstructed representations, the features retain the flexibility needed to adapt to variations introduced by the T_{t+1} while preserving critical information for the previous task. So after training task T_t and obtaining the shared parameters θ_s and task-specific parameters θ_t , we train an under-complete AE with the following minimization objective loss function problem (See part (6) of Fig. 1):

$$\begin{aligned} \arg \min_R \mathbb{E}_{(X_t, Y_t)} \left[\Omega \left\| R(\theta_s(X_t)) - \theta_s(X_t) \right\|_2^2 \right. \\ \left. + \mathcal{L}_{\text{CE}} \left(\theta_t \left(R(\theta_s(X_t)) \right), Y_t \right) \right], \end{aligned} \quad (17)$$

where Ω is a hyperparameter. We use the encoder weights for better memory usage as they are for lower dimensions

and can be calculated before training the T_{t+1} . In the subsequent steps, we adopt the same stepwise freezing approach utilized in the NFL framework. Specifically, steps 3, 4, and 5 in the algorithm 2 are analogous to steps 2, 3, and 4 of the algorithm 1, with the key distinction of using unbiased logits to enhance model performance.

For the last step to address the bias in logits caused by the imbalance between the number of samples in old and new classes, we apply a transformation to correct the bias. This transformation is defined as follows:

$$\Gamma(X_{t+1}) = w_{\text{bias}}W_{\text{Enc}}X_{t+1} + b_{\text{bias}} \quad (18)$$

$$H'_t = \Gamma(X_{t+1})H_t. \quad (19)$$

Here, w_{bias} and b_{bias} are in the same dimension with W_{Enc} . These parameters are trained using a cross-validation set to adjust the encoded feature representations. Notably, all other parameters of the model remain frozen during this process. The minimization function for training bias correction layer is in the following:

$$\mathbb{E}_{\text{bias}} \left[\left\| \Gamma(X_{t+1}) - \mathbf{1} \right\|_2^2 \right]. \quad (20)$$

This promotes unbiased learning by guiding the transformation function to remain close to the identity mapping. The minimization objective function for training the AE is:

$$\mathbb{E}_{\text{AE}} \left[\left\| \sigma \left(W_{\text{Enc}}\theta_s^r(X_{t+1}) \right) - \sigma \left(W_{\text{Enc}}\theta_s(X_{t+1}) \right) \right\|_2^2 \right]. \quad (21)$$

We use Eq. 13 and Eq. 14 for calculating the NN_5 outputs. The final loss function for training NFL+ is:

$$\begin{aligned} \mathcal{L}'_5 = & \mathbb{E} \left[\eta \mathcal{L}_{\text{KD}} \left(H'_t, O_t^5 \right) + (1 - \eta) \mathcal{L}_{\text{KD}} \left(\tilde{H}_t, O_t^5 \right) \right. \\ & + \phi \mathcal{L}_{\text{CE}} \left(Y_{t+1}, O_{t+1}^5 \right) + \rho \left\| \sigma \left(W_{\text{Enc}}\theta_s^r(X_{t+1}) \right) \right. \\ & \left. \left. - \sigma \left(W_{\text{Enc}}\theta_s(X_{t+1}) \right) \right\|_2^2 + \tau \left\| \Gamma(X_{t+1}) - \mathbf{1} \right\|_2^2 \right], \end{aligned} \quad (22)$$

where ϕ , ρ , η and τ are hyperparameters. Multiple loss function terms strike a good balance between learning new tasks and preventing forgetting.

4. Experiments

Scenarios: We conducted a series of experiments to evaluate the performance of the NFL in Task Incremental Learning (Task-IL) and Class Incremental Learning (Class-IL) scenarios (See details in supplementary material).

Evaluation Metrics: To assess the ability of each method to perform effective CL and battle CF, we use Average Accuracy (ACC), Forward transfer (FWT), Backward transfer (BWT) for Task-IL scenario and ACC, Average Forgetting (AF), and Intransigence (I) for Class-IL scenario. When CL

Algorithm 2: NFL+

Inputs: Dataset $D_{t+1}(X_{t+1}, Y_{t+1})$ describing T_{t+1} , Parameters $\{\theta_s, \theta_t\}$ trained on T_t

Step 1: Corresponding to NFL's Step 1

Step 2: Train AE for Feature Preservation

$$\begin{aligned} \arg \min_R \mathbb{E}_{(X_t, Y_t)} \left[\Omega \left\| R \left(\theta_s(X_t) \right) - \theta_s(X_t) \right\|_2^2 \right. \\ \left. + \mathcal{L}_{\text{CE}} \left(\theta_t \left(R \left(\theta_s(X_t) \right) \right), Y_t \right) \right] \end{aligned}$$

Step 3-5: Corresponding to NFL's steps 2-4, respectively

Step 6: Adjust Logit for Bias Correction with Eq. 19, Train NN_5 with \mathcal{L}'_5 from Eq. 22

$$\begin{aligned} \text{NN}_5 \left(X_{t+1}, \theta_s^f, \theta_t, \theta_t^u, \theta_{t+1}^u \right) \rightarrow < O_t^5, (\theta_s^{f+}, \theta_t) >; \\ < O_t^5, (\theta_s^f, \theta_t^f) >; < O_{t+1}^5, (\theta_s^{f+}, \theta_{t+1}^f) > \end{aligned}$$

Output: Share Parameters $\{\theta_s^{f+}\}$, Task Specific Parameters $\{\theta_t^f, \theta_{t+1}^f\}$ for the next task

methods trained for task T_k on D_k , its accuracy on all tasks is measured using the corresponding test sets, leading to a matrix $A \in \mathbb{A}^{T \times T}$ containing the accuracies on all T tasks, i.e., $A_{i,j}$ denotes the accuracy of the model on task T_j after trained completely on task T_i .

Average Accuracy (ACC) [25]: This metric assesses the overall performance of the CL method after completing the training of all T tasks.

$$\text{ACC}_T = \frac{1}{T} \sum_{k=1}^T A_{T,k}. \quad (23)$$

Forward transfer (FWT) [25]: which is the influence that training on a k -th task has, on average, on the performance of the model on the next task:

$$\text{FWT}_T = \frac{1}{T-1} \sum_{k=2}^T (A_{k-1,k} - b_k) \quad (24)$$

Here, b_k is the classification accuracy of a randomly initialized reference model for the k -th task.

Backward transfer (BWT) [25]: This metric evaluates the average influence of learning the T -th task on previous tasks:

$$\text{BWT}_T = \frac{1}{T-1} \sum_{k=1}^{T-1} (A_{T,k} - A_{k,k}). \quad (25)$$

Average forgetting (AF) [5]: It measures how much knowledge has been forgotten across the first $T-1$ tasks

in Task-IL (or classes in Class-IL):

$$\text{AF}_T = \frac{1}{T-1} \sum_{j=1}^{T-1} f_T^j, \quad (26)$$

$$f_T^j = \max_{i \in \{1, \dots, T-1\}} A_{i,j} - A_{T,j}, \quad \forall j < T. \quad (27)$$

Intransience measure (I) [5]: It measures the impact on the model’s accuracy when trained in a CL manner compared to training it using the typical batch learning:

$$I_T = A_T^* - A_{T,T}. \quad (28)$$

Here, A_T^* denotes the model’s accuracy if it was trained on the dataset $\mathcal{D} = \cup_{t=1}^T \mathcal{D}_t$.

In addition, we proposed a new metric: the Plasticity-Stability Ratio (PS). Effective CL requires a balance between plasticity, which allows the system to acquire new knowledge, and stability, which ensures that previously learned knowledge is retained. It is of significant importance to strike a good balance between them for effective CL [40]. Excessive plasticity may cause the system to forget previously learned information, while excessive stability can hinder its ability to learn anything new [35, 37]. Our proposed metric assesses how well CL methods scale with the increasing number of tasks and classes.

Plasticity-Stability (PS): This metric quantifies the trade-off between plasticity and stability:

$$\text{PS}_T = \frac{1}{T-1} \frac{\sum_{k=2}^T (A_{k,k} - A_{k-1,k})}{\left| \sum_{k=1}^{T-1} A_{T,k} - A_{k,k} \right|}. \quad (29)$$

To summarize, for a CL method, the higher the ACC, FWT, BWT, and PS, and the lower the AF and I in the trained models, the better the method is at combating CF [9]. If two models have similar ACC, the one with a larger PS, BWT, and/or FWT is preferable. Notably, Backward transfer for the first task and forward transfer for the last task are meaningless [25].

Datasets: Table 1 provides an overview of the datasets utilized for evaluation.

Table 1. Summary of datasets and task splits

Dataset	Classes	Tasks for Task-IL	Classes for Class-IL
CIFAR-100 [18]	100	10	10
TinyImageNet [20]	200	10	20
ImageNet-1000 [19]	1,000	10	100

Methods: We compare NFL and NFL+ performance with other CL methods, and their characteristics are summarized

in Table 2. We used Stochastic Gradient Descent (SGD) as a lower bound and joint training as an upper bound to establish performance bounds.

Table 2. Comparison methods characteristics.

Method	Knowledge Distillation-Based	Memory Based	Dynamic Network
NFL (Ours)	✓	✗	✗
NFL+ (Ours)	✓	✗	✗
LwF [22]	✓	✗	✗
Coil [47]	✓	✓	✗
iCaRL [30]	✓	✓	✗
DER++ [3]	✓	✓	✗
MEMO [48]	✗	✓	✓

4.1. Experiment Setup and Results

For the experiments on the CIFAR-100, TinyImageNet, and ImageNet-1000 datasets, we employ the ResNet-18 [13]. The initialization [12] is applied to these layers, as it is well-suited for ReLU activations, ensuring stable gradient propagation across layers. All models were trained using the SGD optimizer to maintain consistency across different CL methods. Additionally, all hyperparameters were carefully fine-tuned through a grid search to optimize performance. For the Class-IL scenario, we set the number of exemplars to 2,000 for both CIFAR-100 and TinyImageNet and 20,000 for ImageNet-1000 [50]. For the Task-IL scenario, we set 200, 500, and 5120 exemplars for all datasets [3]. Notably, the NFL and NFL+ do not need to have exemplars.

We evaluate CL methods across multiple datasets by structuring learning into $T = 10$ sequential tasks, where each data instance is encountered only once during training. The results, summarized in Table 3, assess model performance under this constraint for the Task-IL scenario. Additionally, we conduct experiments on CIFAR-100, TinyImageNet, and ImageNet-1000, respectively, for the Class-IL scenario with results presented in Fig. 2, Fig. 3, and Fig. 4 respectively. Moreover, Table 4 provides additional metrics for CIFAR-100 with 10 incremental classes in the Class-IL scenario (See supplementary material for other datasets). These experiments provide insights into the scalability of CL methods across datasets of varying complexity. More results and visualizations are provided in the supplementary material.

We evaluate the total memory cost of ResNet-18 on ImageNet-1000 by summing the memory required for storing exemplars and model parameters. Each ImageNet-1000 exemplar requires $3 \times 224 \times 224 = 150,528$ bytes. With 20,000 exemplars, the total memory footprint for stored images is approximately 3,010.56 MB across exemplar-based methods, e.g., Coil, iCaRL, DER++, and MEMO. The model memory varies based on the number of model

Table 3. Performance of CL methods for Task-IL scenario on CIFAR-100, TinyImageNet, and ImageNet-1000 averaged over ten runs. The symbol “-” indicates experiments not conducted due to incompatibilities.

Buffer	Method	ACC			FWT			BWT		
		CIFAR-100	TinyImageNet	ImageNet-1000	CIFAR-100	TinyImageNet	ImageNet-1000	CIFAR-100	TinyImageNet	ImageNet-1000
—	NFL (Ours)	83.45 ± 1.25	49.77 ± 5.38	46.19 ± 3.55	8.51 ± 4.90	8.02 ± 5.13	6.51 ± 5.32	-9.22 ± 8.49	-14.73 ± 9.41	-23.62 ± 8.57
—	NFL+ (Ours)	92.68 ± 2.45	58.21 ± 4.10	54.13 ± 3.19	13.98 ± 7.29	9.41 ± 6.71	7.31 ± 5.02	-0.35 ± 7.45	-1.35 ± 5.56	-5.19 ± 7.16
—	Upper Bound	97.4 ± 0.12	89.26 ± 1.40	84.26 ± 1.26	-	-	-	-	-	-
—	Lower Bound	58.41 ± 4.17	28.92 ± 2.978	21.54 ± 1.58	-3.06 ± 2.90	-8.21 ± 3.74	-11.09 ± 4.01	-55.39 ± 10.12	-64.61 ± 14.98	-79.24 ± 12.12
—	LwF	62.86 ± 3.50	25.85 ± 1.59	26.07 ± 2.59	1.39 ± 4.06	0.97 ± 7.26	0.63 ± 5.12	-39.69 ± 10.25	-41.21 ± 8.54	-58.59 ± 10.28
200	Coil	77.99 ± 3.92	42.62 ± 2.81	35.89 ± 4.63	-1.26 ± 2.22	-4.17 ± 3.47	-6.39 ± 4.30	-6.40 ± 12.67	-9.78 ± 6.31	-14.36 ± 10.03
200	iCaRL	81.14 ± 2.13	45.19 ± 2.44	37.27 ± 3.44	-	-	-	-2.72 ± 10.20	-7.25 ± 5.01	-10.01 ± 4.14
200	DER++	84.45 ± 2.60	51.50 ± 3.64	47.27 ± 2.78	-0.69 ± 1.86	-2.50 ± 5.13	-5.88 ± 6.90	-8.59 ± 3.32	-14.10 ± 13.21	-15.16 ± 10.21
200	MEMO	84.63 ± 1.99	53.14 ± 3.29	48.76 ± 4.63	-0.09 ± 2.09	-1.95 ± 3.75	-3.69 ± 2.04	-2.39 ± 6.00	-3.82 ± 7.77	-5.88 ± 9.61
500	Coil	81.25 ± 4.01	43.70 ± 1.97	40.19 ± 6.20	-0.27 ± 2.80	-1.57 ± 6.30	-4.23 ± 8.35	-4.13 ± 11.34	-7.96 ± 9.51	-11.16 ± 8.35
500	iCaRL	86.93 ± 3.61	48.21 ± 3.76	39.44 ± 2.91	-	-	-	-5.71 ± 1.10	-9.49 ± 3.53	-13.06 ± 4.55
500	DER++	88.45 ± 3.59	53.61 ± 4.11	49.27 ± 3.09	1.90 ± 2.07	-0.11 ± 2.17	-1.29 ± 3.00	-2.38 ± 1.46	-4.50 ± 5.81	-5.66 ± 7.15
500	MEMO	89.01 ± 4.13	53.75 ± 3.33	50.19 ± 3.63	0.29 ± 2.23	-0.65 ± 4.44	-0.97 ± 2.56	-2.36 ± 2.00	-4.36 ± 3.27	-5.10 ± 4.46
5120	Coil	86.27 ± 3.33	46.21 ± 2.32	44.19 ± 4.63	2.71 ± 1.05	0.16 ± 3.46	-1.23 ± 2.67	-1.24 ± 11.44	-5.24 ± 5.37	-7.55 ± 4.90
5120	iCaRL	89.26 ± 3.22	49.03 ± 5.01	44.03 ± 2.97	-	-	-	-4.94 ± 4.10	-8.64 ± 3.47	-9.87 ± 3.81
5120	DER++	90.45 ± 3.61	56.31 ± 4.96	53.27 ± 2.79	3.71 ± 2.00	2.76 ± 1.11	1.23 ± 0.63	-1.33 ± 9.14	-2.98 ± 6.44	-3.10 ± 8.15
5120	MEMO	90.87 ± 3.41	58.19 ± 3.85	54.19 ± 2.63	10.25 ± 6.63	8.19 ± 4.26	7.76 ± 5.13	-1.56 ± 9.39	-2.18 ± 5.71	-4.18 ± 4.00

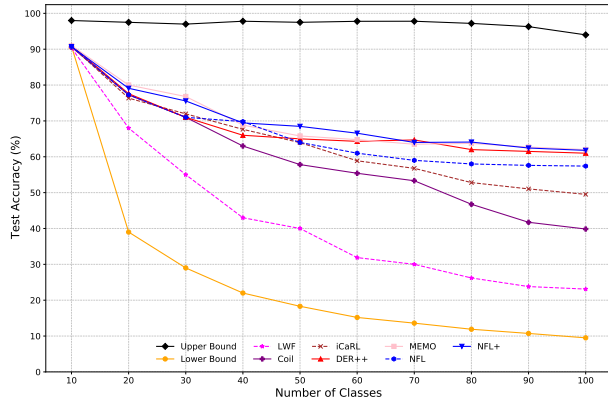


Figure 2. ACC comparison for Class-IL using CIFAR-100 (10 incremental classes per task).

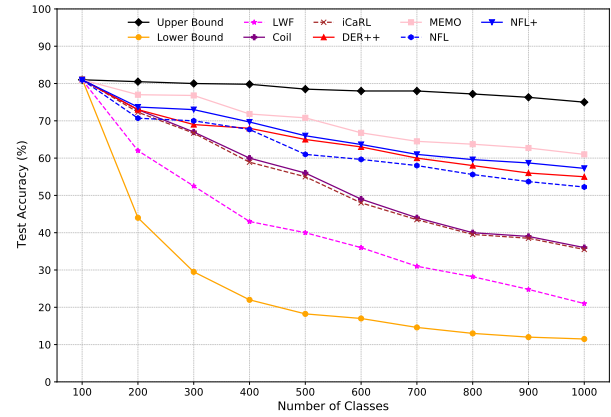


Figure 4. ACC comparison for Class-IL using ImageNet-1000 (100 incremental classes per task).

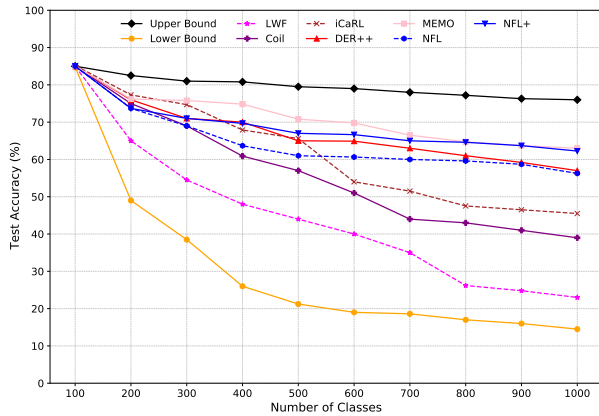


Figure 3. ACC comparison for Class-IL using TinyImageNet (20 incremental classes per task).

parameters. Each parameter is stored as a 32-bit float (4 bytes). Most methods, including LwF, iCaRL, Coil,

Table 4. ACC, AF, I, and PS measure on CIFAR-100 for Class-IL scenario with 10 incremental classes.

Method	ACC	AF	I	PS
NFL (Ours)	66.59	0.3059	-0.0092	0.3891
NFL+ (Ours)	70.22	0.1119	-0.0101	0.4573
LwF	43.14	0.4443	-0.0280	0.3888
Coil	59.67	0.2880	-0.0143	0.3926
iCaRL	63.97	0.2243	-0.0031	0.3263
DER++	68.41	0.1091	0.0129	0.2667
MEMO	69.92	0.2043	0.0025	0.2241

DER++, and NFL, contain 11.17 Million (M) parameters, hence requiring 44.68 MB, while NFL+ has 11.56 M parameters (i.e. 46.24 MB). MEMO, with 170.6 M parameters, is the most memory-intensive, requiring 682.4 MB. Overall, for memory-based methods, the total memory consumption ranges from 3,055.24 MB to 3,692.96 MB. Fig. 5

illustrates the memory footprint of each method.

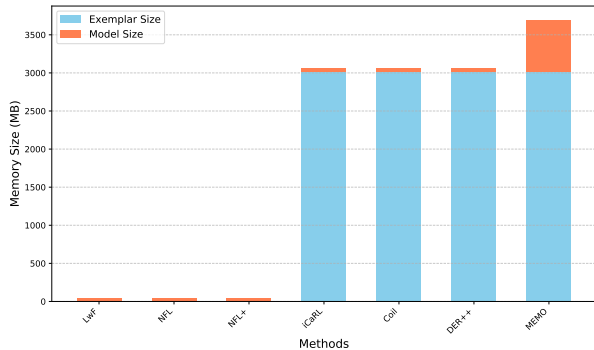


Figure 5. Memory size for ImageNet-1000 for different comparison methods. Blue bars denote the memory budget for exemplars, and orange bars denote the memory budget for keeping the model.

4.2. Discussions

4.2.1. Comparison on Small-Scale Datasets

As shown in Fig. 2 and Table 3, NFL+ achieves better or comparable performance in both Class-IL and Task-IL settings, particularly comparing the results with MEMO, a dynamic architecture-based approach. While MEMO achieves better performance for the ImageNet-1000 dataset, it achieves this at the cost of significantly larger model sizes, raising concerns about computational scalability. Further analysis of logit-based methods such as Coil, iCaRL, and DER++ reveals that their performance improvement over memory-free methods like LwF attributes to using buffer exemplars to enhance knowledge retention. In particular, DER++ benefits from its training trajectory representation within a functional L^2 Hilbert space, effectively preserving past knowledge. In contrast, LwF, a knowledge distillation-based method, exhibits the lowest performance, primarily due to its lack of exemplar storage, which limits its ability to retain prior knowledge. As shown in Table 3, the performance of memory-based methods improves proportionally with buffer size.

Notably, NFL+ leverages a stepwise freezing strategy to consolidate knowledge from previous tasks while facilitating adaptation to new ones. With this novel training method, NFL+ outperforms most memory-based approaches, including Coil, iCaRL, and DER++, despite not having access to previous exemplars. However, despite these improvements, Fig. 2 and Fig. 3 show a persistent performance gap between CL methods and the upper bound achieved by joint training. This underscores a fundamental challenge in CL: existing methodologies struggle to achieve optimal classification accuracy, necessitating more efficient knowledge retention and transfer strategies.

4.2.2. Comparison on large-Scale Datasets

As shown in Fig. 3 and Fig. 4, the performance trends across most methods are aligned with those observed on CIFAR-100. Notably, NFL+ achieves substantial improvements, comparable to MEMO, despite requiring 14.75 times less memory. This contrast underscores a fundamental issue in CL evaluation: the unfair comparison of methods with vastly different memory footprints. Dynamic architectures inherently allocate additional model memory resources, providing a clear advantage over methods such as LwF, NFL, and NFL+, which do not utilize exemplar buffers. As discussed in Section 1, a core principle of CL is the strict absence of access to past task data, which challenges the validity of current evaluation frameworks. To mitigate this unfair comparison, the authors in [50] proposed increasing the exemplar capacity for memory-based approaches. However, this adjustment is incompatible with LwF, NFL, and NFL+ methods, which fundamentally do not store exemplars. Additionally, even for memory-based methods like iCaRL and Coil, simply expanding the exemplar set does not sufficiently bridge the gap caused by the higher memory requirements of dynamic architectures.

These findings highlight the urgent need for a more equitable benchmarking framework that systematically accounts for differences in memory consumption, model complexity, and data access constraints. Without such adjustments, existing evaluation paradigms may lead to misleading conclusions about the effectiveness of different CL approaches.

5. Conclusion

We introduced NFL and its enhanced variant, NFL+. NFL employs knowledge distillation to mitigate CF by preserving prior knowledge through soft-target supervision. Building upon this foundation, NFL+ integrates an under-complete AE to retain essential feature representations. NFL+ ensures **knowledge retention**, **bias minimization**, and **stepwise freezing** for incremental learning settings.

We propose the Plasticity-Stability Ratio to improve the evaluation of CL models. Extensive benchmarking demonstrates that NFL and NFL+ achieve an effective balance between learning new tasks and preserving performance on previous ones. Their performance exhibited by memory-free CL frameworks represents a scalable and efficient alternative to conventional approaches.

References

- [1] Rahaf Aljundi, Punarjay Chakravarty, and Tinne Tuytelaars. Expert gate: Lifelong learning with a network of experts. In *CVPR*, 2017. 2
- [2] Rahaf Aljundi, Francesca Babiloni, Mohamed Elhoseiny, Marcus Rohrbach, and Tinne Tuytelaars. Memory Aware Synapses: Learning what (not) to forget. In *ECCV*, 2018. 1

- [3] Pietro Buzzega, Matteo Boschini, Angelo Porrello, Davide Abati, and Simone Calderara. Dark experience for general continual learning: a strong, simple baseline. In *NIPS*, pages 15920–15930, 2020. 1, 2, 6
- [4] Francisco M Castro, Manuel J Marín-Jiménez, Nicolás Guil, Cordelia Schmid, and Karteek Alahari. End-to-end incremental learning. In *ECCV*, pages 233–248, 2018. 2
- [5] Arslan Chaudhry, Puneet K. Dokania, Thalaiyasingam Ajanthan, and Philip H. S. Torr. Riemannian walk for incremental learning: Understanding forgetting and intransigence. In *ECCV*, 2018. 5, 6
- [6] Prithviraj Dhar, Rajat Vikram Singh, Kuan-Chuan Peng, Ziyang Wu, and Rama Chellappa. Learning without memorizing. In *CVPR*, pages 5138–5146, 2019. 2
- [7] Arthur Douillard, Matthieu Cord, Charles Ollion, Thomas Robert, and Eduardo Valle. Podnet: Pooled outputs distillation for small-tasks incremental learning. In *ECCV*, pages 86–102, 2020. 2
- [8] Arthur Douillard, Alexandre Ramé, Guillaume Couairon, and Matthieu Cord. DyTox: Transformers for Continual Learning With DYNAMIC TOken eXpansion. In *CVPR*, pages 9285–9295, 2022. 1
- [9] Natalia Díaz-Rodríguez, Vincenzo Lomonaco, David Filliat, and Davide Maltoni. Don't forget, there is more than forgetting: new metrics for continual learning, 2018. <https://arxiv.org/abs/1810.13166>. 6
- [10] Ian Goodfellow, Yoshua Bengio, and Aaron Courville. *Deep Learning*. MIT Press, 2016. 4
- [11] Jianping Gou, Baosheng Yu, Stephen J Maybank, and Dacheng Tao. Knowledge distillation: A survey. *IJCV*, 129(6):1789–1819, 2021. 2
- [12] Kaiming He, Xiangyu Zhang, Shaoqing Ren, and Jian Sun. Delving deep into rectifiers: Surpassing human-level performance on imagenet classification. In *ICCV*, 2015. 6
- [13] Kaiming He, Xiangyu Zhang, Shaoqing Ren, and Jian Sun. Deep residual learning for image recognition. In *CVPR*, 2016. 6
- [14] Geoffrey Hinton, Oriol Vinyals, and Jeff Dean. Distilling the knowledge in a neural network, 2015. <https://arxiv.org/abs/1503.02531>. 2, 3
- [15] Saihui Hou, Xinyu Pan, Chen Change Loy, Zilei Wang, and Dahua Lin. Learning a unified classifier incrementally via rebalancing. In *CVPR*, pages 831–839, 2019. 2
- [16] Ahmet Iscen, Jeffrey Zhang, Svetlana Lazebnik, and Cordelia Schmid. Memory-efficient incremental learning through feature adaptation. In *ECCV*, pages 699–715, 2020. 2
- [17] James Kirkpatrick, Razvan Pascanu, Neil Rabinowitz, Joel Veness, Guillaume Desjardins, Andrei A. Rusu, Kieran Milan, John Quan, Tiago Ramalho, Agnieszka Grabska-Barwinska, Demis Hassabis, Claudia Clopath, Dharshan Kumaran, and Raia Hadsell. Overcoming catastrophic forgetting in neural networks. *Proceedings of the National Academy of Sciences*, 114(13):3521–3526, 2017. 1
- [18] Alex Krizhevsky. Learning multiple layers of features from tiny images. Technical report, University of Toronto, 2009. 6
- [19] Alex Krizhevsky, Ilya Sutskever, and Geoffrey E Hinton. Imagenet classification with deep convolutional neural networks. In *NIPS*, pages 1401–1476, 2012. 6
- [20] Ya Le and Xuan S. Yang. Tiny imagenet visual recognition challenge, 2015. 6
- [21] Kibok Lee, Kimin Lee, Jinwoo Shin, and Honglak Lee. Overcoming catastrophic forgetting with unlabeled data in the wild. In *ICCV*, pages 312–321, 2019. 2
- [22] Zhizhong Li and Derek Hoiem. Learning without forgetting. *PAMI*, 40(12):2935–2947, 2018. 1, 2, 6
- [23] Xialei Liu, Marc Masana, Luis Herranz, Joost Van de Weijer, Antonio M. López, and Andrew D. Bagdanov. Rotate your Networks: Better Weight Consolidation and Less Catastrophic Forgetting. In *ICPR*, pages 2262–2268, 2018. 1
- [24] Yaoyao Liu, Bernt Schiele, and Qianru Sun. RMM: reinforced memory management for class-incremental learning. In *NIPS*, 2024. 2
- [25] David Lopez-Paz and Marc' Aurelio Ranzato. Gradient episodic memory for continual learning. In *NIPS*, 2017. 5, 6
- [26] German I Parisi, Ronald Kemker, Jose L Part, Christopher Kanan, and Stefan Wermter. Continual lifelong learning with neural networks: A review. *Neural Networks*, 113:54–71, 2019. 1
- [27] B. Pfüll and A. Gepperth. A comprehensive, application-oriented study of catastrophic forgetting in DNNs. In *ICLR*, 2019. 1
- [28] Haoxuan Qu, Hossein Rahmani, Li Xu, Bryan Williams, and Jun Liu. Recent Advances of Continual Learning in Computer Vision: An Overview, 2024. <https://arxiv.org/abs/2109.11369>. 1
- [29] Atoum Rannen, Rahaf Aljundi, Matthew B Blaschko, and Tinne Tuytelaars. Encoder-based lifelong learning. In *ICCV*, pages 1320–1328, 2017. 1, 2
- [30] Sylvestre-Alvise Rebuffi, Alexander Kolesnikov, Georg Sperl, and Christoph H. Lampert. icarl: Incremental classifier and representation learning. In *CVPR*, pages 2001–2010, 2017. 1, 2, 6
- [31] Tim GJ Rudner, Freddie Bickford Smith, Qixuan Feng, Yee Whye Teh, and Yarin Gal. Continual learning via sequential function-space variational inference. In *ICML*, pages 18871–18887, 2022. 2
- [32] Andrei A. Rusu, Neil C. Rabinowitz, Guillaume Desjardins, Hubert Soyer, James Kirkpatrick, Koray Kavukcuoglu, Razvan Pascanu, and Raia Hadsell. Progressive Neural Networks, 2022. <https://arxiv.org/abs/1606.04671>. 1
- [33] Gobinda Saha, Isha Garg, and Kaushik Roy. Gradient projection memory for continual learning. In *ICLR*, 2021. 1
- [34] Qing Sun, Fan Lyu, Fanhua Shang, Wei Feng, and Liang Wan. Exploring Example Influence in Continual Learning. In *NIPS*, pages 27075–27086, 2022. 2
- [35] Mohammad Ali Vahedifar, Qi Zhang, and Alexandros Iosifidis. Towards lifelong deep learning: A review of continual learning and unlearning methods, 2025. <https://doi.org/10.5281/zenodo.14631802>. 1, 6
- [36] Eli Verwimp, Rahaf Aljundi, Shai Ben-David, Matthias Bethge, Andrea Cossu, Alexander Gepperth, Tyler L.

- Hayes, Eyke Hüllermeier, Christopher Kanan, Dhireesha Kudithipudi, Christoph H. Lampert, Martin Mundt, Razvan Pascanu, Adrian Popescu, Andreas S. Tolias, Joost van de Weijer, Bing Liu, Vincenzo Lomonaco, Tinne Tuytelaars, and Gido M. van de Ven. Continual learning: Applications and the road forward. *TMLR*, 2024. 1
- [37] Liyuan Wang, Xingxing Zhang, Hang Su, and Jun Zhu. A comprehensive survey of continual learning: theory, method and application. *PAMI*, 46(8):5362–5383, 2024. 6
- [38] Zhen Wang, Liu Liu, Yiqun Duan, and Dacheng Tao. Continual learning through retrieval and imagination. In *AAAI*, 2022. 2
- [39] Zhenyi Wang, Enneng Yang, Li Shen, and Heng Huang. A comprehensive survey of forgetting in deep learning beyond continual learning, 2023. <https://arxiv.org/abs/2307.09218>. 1, 2
- [40] Buddhi Wickramasinghe, Gobinda Saha, and Kaushik Roy. Continual learning: A review of techniques, challenges and future directions. *TNNLS*, pages 123–140, 2024. 6, 1
- [41] Chenshen Wu, Luis Herranz, Xialei Liu, Joost van de Weijer, and Bogdan Raducanu. Memory replay gans: Learning to generate new categories without forgetting. In *NIPS*, 2018. 2
- [42] Yue Wu, Yinpeng Chen, Lijuan Wang, Yuancheng Ye, Zicheng Liu, Yandong Guo, and Yun Fu. Large scale incremental learning. In *CVPR*, 2019. 1, 2
- [43] Jaehong Yoon, Eunho Yang, Jeongtae Lee, and Sung Ju Hwang. Lifelong Learning with Dynamically Expandable Networks. In *ICLR*, 2018. 1
- [44] Guanxiong Zeng, Yang Chen, Bo Cui, and Shan Yu. Continual learning of context-dependent processing in neural networks. *Nature Machine Intelligence*, 1(8):364–372, 2019. 1
- [45] Friedemann Zenke, Ben Poole, and Surya Ganguli. Continual learning through synaptic intelligence. In *ICML*, pages 3987–3995, 2017. 1
- [46] Mengyao Zhai, Lei Chen, Frederick Tung, Jiawei He, Megha Nawhal, and Greg Mori. Lifelong gan: Continual learning for conditional image generation. In *ICCV*, pages 2759–2768, 2019. 2
- [47] Da-Wei Zhou, Han-Jia Ye, and De-Chuan Zhan. Co-Transport for Class-Incremental Learning. In *ACMMM*, page 1645–1654, 2021. 2, 6
- [48] Da-Wei Zhou, Qi-Wei Wang, Han-Jia Ye, and De-Chuan Zhan. A model or 603 exemplars: Towards memory-efficient class-incremental learning. In *ICLR*, 2023. 2, 6
- [49] Da-Wei Zhou, Hai-Long Sun, Jingyi Ning, Han-Jia Ye, and De-Chuan Zhan. Continual Learning with Pre-Trained Models: A Survey. In *IJCAI*, pages 8363–8371, 2024. 1
- [50] Da-Wei Zhou, Qi-Wei Wang, Zhi-Hong Qi, Han-Jia Ye, De-Chuan Zhan, and Ziwei Liu. Class-incremental learning: A survey. *PAMI*, 46(12):9851–9873, 2024. 1, 6, 8

No Forgetting Learning: Memory-free Continual Learning

Supplementary Material

The supplementary material mainly contains additional materials and experiments that cannot be reported due to the page limit, which is organized as follows:

- Section 6 details CL’s main scenarios utilized in this paper.
- Section 7 provides additional results related to more evaluation metrics for Class-IL scenario, and time and memory computational cost.

6. Evaluation Protocol

The two main experimental scenarios typically used to evaluate the performance of methods are the following:

- **Task Incremental Learning (Task-IL):** In Task-IL, the training data is divided into multiple tasks, each with a unique set of classes. The crucial aspect of Task-IL is that the model is provided with information about which task it is handling during training and testing. This allows the model to use the computational graph corresponding to each task. For example, if the model is trained to classify images of animals and vehicles, the task label information is also provided for testing on a new image; thus, the network’s classification output for the corresponding task will be calculated. This knowledge simplifies the inference task, as the model does not need to consider all possible classes simultaneously [35, 40].
- **Class Incremental Learning (Class-IL):** In Class-IL, the model is also trained on different tasks but is not told which task a new sample belongs to during testing. Instead, regardless of the task, the model needs to respond to all the classes it has encountered. This makes Class-IL more challenging than Task-IL, as the model must infer the correct class without task-related information. For instance, after training a model to recognize animals and vehicles separately, Class-IL would test the model on all classes simultaneously (animals and vehicles) without informing the model whether it is currently classifying an animal or a vehicle [28, 49].

7. Additional Results

We report Class-IL for the CIFAR-100 dataset, where all 100 classes were trained under the configuration of 20 tasks, with each corresponding to 5 incremental classes. The result is illustrated in Fig. 6. This helps us understand how the number of tasks or classes affects performance. By comparing it to Fig. 2, we see that performance declines as the number of tasks increases. This raises an important question: for a fixed number of classes, what is the optimal number of tasks to maintain the best performance?

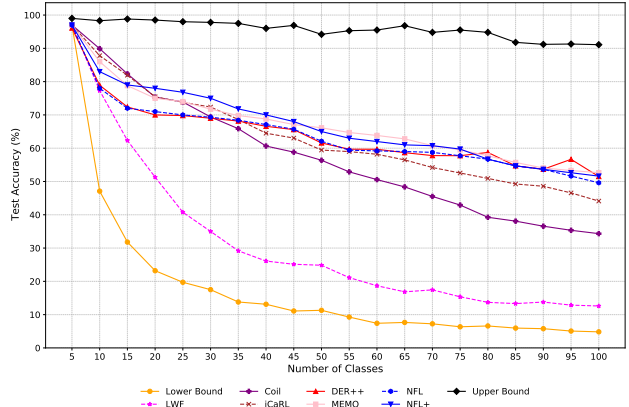


Figure 6. ACC comparison for Class-IL using CIFAR-100 (5 incremental classes per task).

Table 5. ACC, AF, I, and PS measure on CIFAR-100 for Class-IL scenario with 5 incremental classes.

Method	ACC	AF	I	PS
NFL (Ours)	64.05	0.4100	0.0002	0.4689
NFL+ (Ours)	66.97	0.1708	-0.0054	0.5252
LwF	31.23	0.5978	0.0048	0.2105
Coil	57.67	0.3748	-0.0505	0.2752
iCaRL	63.19	0.3348	-0.0212	0.2673
DER++	64.35	0.1841	0.0237	0.3215
MEMO	66.97	0.2876	-0.0147	0.4731

Our findings indicate that methods achieving higher final performance generally exhibit lower levels of forgetting, as shown in Table 5 and illustrated Fig. 6. This correlation arises because the final performance directly affects the second term in the forgetting calculation, underscoring the intrinsic relationship between these metrics. While helping with stability, regularization terms can reduce the model’s ability to adapt to new tasks (plasticity), leading to poorer PS performance. This highlights the importance of the PS metric.

By analyzing Tables 4 and 5, we can observe the ACC across all methods tends to decrease slightly when moving from 10 to 5 incremental classes per task. This is expected as increasing the number of incremental steps generally increases task complexity. However, the NFL+ consistently achieves the highest ACC in both settings (66.97 for five incremental classes per task and 70.22 for ten incremental classes per task), demonstrating its effectiveness. The NFL+ maintains the highest plasticity in both cases (9.98

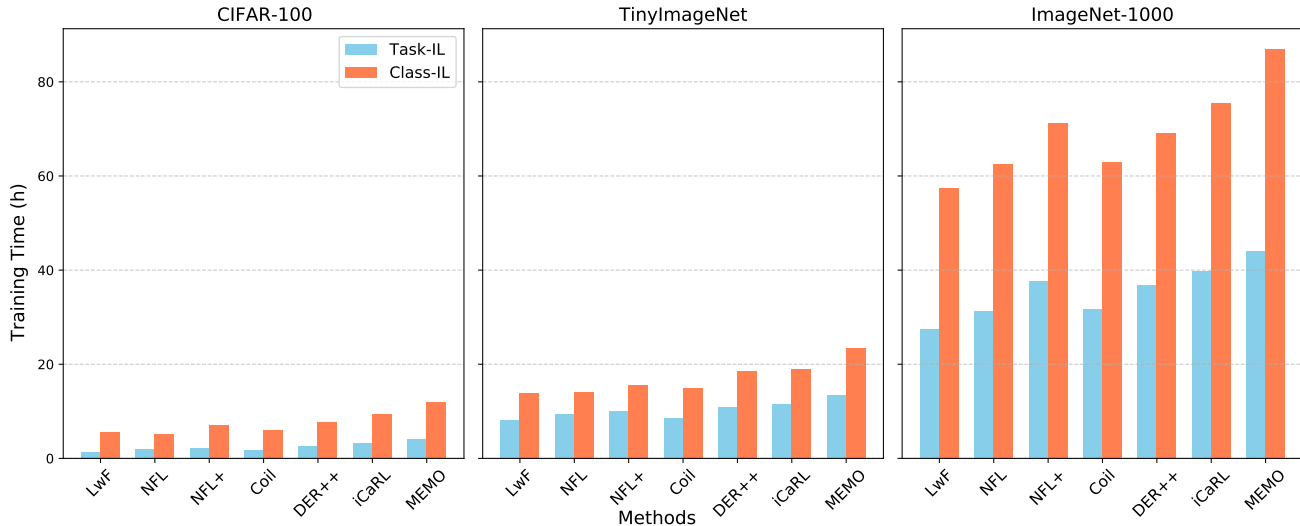


Figure 7. Training time (h) of CIFAR-100, TinyImageNet and ImageNet-1000 Class-IL and Task-IL experiments for all methods, e.g., Coil, DER++, iCaRL, and MEMO (For buffer-based methods, a total of 5120 exemplars are utilized in Task-IL experiments, while Class-IL experiments employ 2000 exemplars for CIFAR-100 and TinyImageNet, and 20,000 exemplars for ImageNet-1000).

for the case of five incremental classes per task and 4.116 for ten incremental classes per task).

For TinyImageNet, ACC is presented in Fig. 3, with additional metrics, ACC, AF, I, and PS, summarized in Table 6. Similarly, for ImageNet-1000, ACC is illustrated in Fig. 4, while Table 7 summarizes the ACC, AF, I, and PS metrics. The performance trends across most methods align with those observed on CIFAR-100. However, on large-scale datasets, the performance of these methods deteriorates as the number of classes that must be learned in each task increases.

The comparative time benchmarks for each method are presented in Fig. 7 for all three datasets. The figure illustrates that increasing the number of exemplars enhances performance; however, this improvement comes at the cost of a significant increase in training time. Therefore, developing more computationally efficient algorithms is essential when computational resources are constrained—such as limited iterations or update time.

Table 6. ACC, AF, I, and PS measure on TinyImageNet for Class-IL scenario with 20 incremental classes.

Method	ACC	AF	I	PS
NFL (Ours)	64.76	0.5763	-0.0007	0.6933
NFL+ (Ours)	68.86	0.4866	-0.0027	0.8811
LwF	44.55	0.6195	0.0013	0.2233
Coil	56.49	0.5356	-0.0002	0.3967
iCaRL	61.57	0.5300	-0.0024	0.4233
DER++	67.21	0.4672	0.0003	0.4500
MEMO	71.03	0.5191	-0.0007	0.8000

Table 7. ACC, AF, I, and PS measure on ImageNet-1000 for Class-IL scenario with 100 incremental classes.

Method	ACC	AF	I	PS
NFL (Ours)	62.96	0.4880	0.5491	0.3067
NFL+ (Ours)	66.36	0.3807	0.1307	0.5767
LwF	41.95	0.8013	0.0920	0.1611
Coil	54.50	0.7319	-0.2014	0.3656
iCaRL	53.91	0.4924	-0.2028	0.3344
DER++	64.80	0.3033	0.2338	0.5933
MEMO	69.62	0.4087	0.5541	0.5967